Flexible terabit/s Nyquist-WDM super-channels using a gain-switched comb source

Joerg Pfeifle,[1] Vidak Vujicic,[2] Regan T. Watts,[2] Philipp C. Schindler,[1] Claudius Weimann,[1] Rui Zhou,[2] Wolfgang Freude,[1,3] Liam P. Barry,[2] Christian Koos[1,3,*]

[1]*Institute of Photonics and Quantum Electronics (IPQ), Karlsruhe Institute of Technology (KIT), Germany*
[2]*The Rince Institute, School of Electronic Engineering, Dublin City University (DCU), Ireland*
[3]*Institute of Microstructure Technology (IMT), Karlsruhe Institute of Technology (KIT), Germany*
[*]*christian.koos@kit.edu*

Abstract: Terabit/s super-channels are likely to become the standard for next-generation optical networks and optical interconnects. A particularly promising approach exploits optical frequency combs for super-channel generation. We show that injection locking of a gain-switched laser diode can be used to generate frequency combs that are particularly well suited for terabit/s super-channel transmission. This approach stands out due to its extraordinary stability and flexibility in tuning both center wavelength and line spacing. We perform a series of transmission experiments using different comb line spacings and modulation formats. Using 9 comb lines and 16QAM signaling, an aggregate line rate (net data rate) of 1.296 Tbit/s (1.109 Tbit/s) is achieved for transmission over 150 km of standard single mode fiber (SSMF) using a spectral bandwidth of 166.5 GHz, which corresponds to a (net) spectral efficiency of 7.8 bit/s/Hz (6.7 bit/s/Hz). The line rate (net data rate) can be boosted to 2.112 Tbit/s (1.867 Tbit/s) for transmission over 300 km of SSMF by using a bandwidth of 300 GHz and QPSK modulation on the weaker carriers. For the reported net data rates and spectral efficiencies, we assume a variable overhead of either 7% or 20% for forward- error correction depending on the individual sub-channel quality after fiber transmission.

OCIS codes: (060.0060) Fiber optics and optical communications; (060.1660) Coherent communications; (140.3520) Lasers, injection-locked; (140.3518) Lasers, frequency modulated.

References and links

1. P. Winzer, "Beyond 100G Ethernet," IEEE Commun. Mag. **48**(7), 26–30 (2010).
2. C. R. Cole, "100-Gb/s and beyond transceiver technologies," Opt. Fiber Technol. **17**(5), 472–479 (2011).
3. S. Gringeri, E. Basch, and T. Xia, "Technical considerations for supporting data rates beyond 100 Gb/s," IEEE Commun. Mag. **50**(2), s21–s30 (2012).
4. W. Shieh and I. Djordjevic, *OFDM for Optical Communications* (Elsevier Academic Press, 2010).
5. D. Hillerkuss, R. Schmogrow, T. Schellinger, M. Jordan, M. Winter, G. Huber, T. Vallaitis, R. Bonk, P. Kleinow, F. Frey, M. Roeger, S. Koenig, A. Ludwig, A. Marculescu, J. Li, M. Hoh, M. Dreschmann, J. Meyer, S. Ben Ezra, N. Narkiss, B. Nebendahl, F. Parmigiani, P. Petropoulos, B. Resan, A. Oehler, K. Weingarten, T. Ellermeyer, J. Lutz, M. Moeller, M. Huebner, J. Becker, C. Koos, W. Freude, and J. Leuthold, "26 Tbit s^{-1} line-rate super-channel transmission utilizing all-optical fast Fourier transform processing," Nat. Photonics **5**(6), 364–371 (2011).
6. J. Yu, Z. Dong, J. Zhang, X. Xiao, H.-C. Chien, and N. Chi, "Generation of coherent and frequency-locked multi-carriers using cascaded phase modulators for 10 Tb/s optical transmission system," J. Lightwave Technol. **30**(4), 458–465 (2012).
7. H.-C. Chien, J. Yu, Z. Jia, Z. Dong, and X. Xiao, "Performance assessment of noise-suppressed Nyquist-WDM for terabit superchannel transmission," J. Lightwave Technol. **30**(24), 3965–3971 (2012).
8. R. Schmogrow, M. Winter, M. Meyer, D. Hillerkuss, S. Wolf, B. Baeuerle, A. Ludwig, B. Nebendahl, S. Ben-Ezra, J. Meyer, M. Dreschmann, M. Huebner, J. Becker, C. Koos, W. Freude, and J. Leuthold, "Real-time Nyquist pulse generation beyond 100 Gbit/s and its relation to OFDM," Opt. Express **20**(1), 317–337 (2012).

#212650 - $15.00 USD Received 26 May 2014; revised 25 Aug 2014; accepted 23 Dec 2014; published 13 Jan 2015

9. D. Hillerkuss, R. Schmogrow, M. Meyer, S. Wolf, M. Jordan, P. Kleinow, N. Lindenmann, P. Schindler, A. Melikyan, X. Yang, S. Ben-Ezra, B. Nebendahl, M. Dreschmann, J. Meyer, F. Parmigiani, P. Petropoulos, B. Resan, A. Oehler, K. Weingarten, L. Altenhain, T. Ellermeyer, M. Moeller, M. Huebner, J. Becker, C. Koos, W. Freude, and J. Leuthold, "Single-Laser 32.5 Tbit/s Nyquist WDM Transmission," J. Opt. Commun. Netw. **4**(10), 715–723 (2012).
10. G. Bosco, V. Curri, A. Carena, P. Poggiolini, and F. Forghieri, "On the performance of Nyquist-WDM terabit superchannels based on PM-BPSK, PM-QPSK, PM-8QAM or PM-16QAM subcarriers," J. Lightwave Technol. **29**(1), 53–61 (2011).
11. Y.-K. Huang, E. Mateo, M. Sato, D. Qian, F. Yaman, T. Inoue, Y. Inada, S. Zhang, Y. Aono, T. Tajima, T. Ogata, and Y. Aoki, "Real-time transoceanic transmission of 1-Tb/s Nyquist superchannel at 2.86-b/s/Hz spectral efficiency," in Asia Communications and Photonics Conference, (Optical Society of America, 2012), Paper PAF4C.2.
12. X. Liu, D. Gill, S. Chandrasekhar, L. Buhl, M. Earnshaw, M. Cappuzzo, L. Gomez, Y. Chen, F. Klemens, E. Burrows, Y.-K. Chen, and R. Tkach, "Multi-carrier coherent receiver based on a shared optical hybrid and a cyclic AWG array for terabit/s optical transmission," IEEE Photon. J. **2**(3), 330–337 (2010).
13. C. Weimann, P. C. Schindler, R. Palmer, S. Wolf, D. Bekele, D. Korn, J. Pfeifle, S. Koeber, R. Schmogrow, L. Alloatti, D. Elder, H. Yu, W. Bogaerts, L. R. Dalton, W. Freude, J. Leuthold, and C. Koos, "Silicon-organic hybrid (SOH) frequency comb sources for terabit/s data transmission," Opt. Express **22**(3), 3629–3637 (2014).
14. X. Liu, S. Chandrasekhar, X. Chen, P. J. Winzer, Y. Pan, T. F. Taunay, B. Zhu, M. Fishteyn, M. F. Yan, J. M. Fini, E. M. Monberg, and F. V. Dimarcello, "1.12-Tb/s 32-QAM-OFDM superchannel with 8.6-b/s/Hz intrachannel spectral efficiency and space-division multiplexed transmission with 60-b/s/Hz aggregate spectral efficiency," Opt. Express **19**(26), B958–B964 (2011).
15. J. Pfeifle, V. Brasch, M. Lauermann, Y. Yu, D. Wegner, T. Herr, K. Hartinger, P. Schindler, J. Li, D. Hillerkuss, R. Schmogrow, C. Weimann, R. Holzwarth, W. Freude, J. Leuthold, T. J. Kippenberg, and C. Koos, "Coherent terabit communications with microresonator Kerr frequency combs," Nat. Photonics **8**(5), 375–380 (2014).
16. A. Gnauck, B. Kuo, E. Myslivets, R. Jopson, M. Dinu, J. Simsarian, P. Winzer, and S. Radic, "Comb-based 16-QAM transmitter spanning the C and L bands," IEEE Photon. Technol. Lett. **26**(8), 821–824 (2014).
17. E. Temprana, V. Ataie, B. P.-P. Kuo, E. Myslivets, N. Alic, and S. Radic, "Low-noise parametric frequency comb for continuous C-plus-L-band 16-QAM channels generation," Opt. Express **22**(6), 6822–6828 (2014).
18. V. Ataie, E. Temprana, L. Liu, Y. Myslivets, P. P. Kuo, N. Alic, and S. Radic, "Flex-grid compatible ultra wide frequency comb source for 31.8 Tb/s coherent transmission of 1520 UDWDM channels," in Optical Fiber Communication Conference: Postdeadline Papers, (Optical Society of America, 2014), Paper Th5B.7.
19. A. Mishra, R. Schmogrow, I. Tomkos, D. Hillerkuss, C. Koos, W. Freude, and J. Leuthold, "Flexible RF-based comb generator," IEEE Photon. Technol. Lett. **25**(7), 701–704 (2013).
20. D. Hillerkuss, T. Schellinger, M. Jordan, C. Weimann, F. Parmigiani, B. Resan, K. Weingarten, S. Ben-Ezra, B. Nebendahl, C. Koos, W. Freude, and J. Leuthold, "High-quality optical frequency comb by spectral slicing of spectra broadened by SPM," IEEE Photon. J. **5**(5), 7201011 (2013).
21. P. M. Anandarajah, R. Maher, Y. Xu, S. Latkowski, J. O'Carroll, S. G. Murdoch, R. Phelan, J. O'Gorman, and L. Barry, "Generation of coherent multicarrier signals by gain switching of discrete mode lasers," IEEE Photon. J. **3**(1), 112–122 (2011).
22. P. Anandarajah, R. Zhou, R. Maher, D. M. Gutierrez Pascual, F. Smyth, V. Vujicic, and L. Barry, "Flexible optical comb source for super channel systems," in Optical Fiber Communication Conference/National Fiber Optic Engineers Conference 2013, (Optical Society of America, 2013), Paper OTh3I.8.
23. R. Zhou, S. Latkowski, J. O'Carroll, R. Phelan, L. P. Barry, and P. Anandarajah, "40 nm wavelength tunable gain-switched optical comb source," Opt. Express **19**(26), B415–B420 (2011).
24. P. M. Anandarajah, R. Zhou, R. Maher, D. Lavery, M. Paskov, B. Thomsen, S. Savory, and L. P. Barry, "Gain-switched multicarrier transmitter in a long-reach UDWDM PON with a digital coherent receiver," Opt. Lett. **38**(22), 4797–4800 (2013).
25. R. Zhou, P. Anandarajah, R. Maher, M. Paskov, D. Lavery, B. Thomsen, S. Savory, and L. Barry, "80-km coherent DWDM-PON on 20-GHz grid with injected gain switched comb source," IEEE Photon. Technol. Lett. **26**(4), 364–367 (2014).
26. V. Vujicic, J. Pfeifle, R. Watts, P. C. Schindler, C. Weimann, R. Zhou, W. Freude, C. G. Koos, and L. Barry, "Flexible terabit/s Nyquist-WDM superchannels with net SE > 7bit/s/Hz using a gain-switched comb source," in Proceedings of CLEO: 2014, (Optical Society of America, 2014), Paper SW1J.3.
27. G. Yabre, H. de Waardt, H. P. A. Van den Boom, and G.-D. Khoe, "Noise characteristics of single-mode semiconductor lasers under external light injection," IEEE J. Quantum Electron. **36**(3), 385–393 (2000).
28. R. Zhou, T. N. Huynh, V. Vujicic, P. M. Anandarajah, and L. P. Barry, "Phase noise analysis of injected gain switched comb source for coherent communications," Opt. Express **22**(7), 8120–8125 (2014).
29. R. Zhou, P. M. Anandarajah, D. Gutierrez Pascual, J. O'Carroll, R. Phelan, B. Kelly, and L. P. Barry, "Monolithically integrated 2-section lasers for injection locked gain switched comb generation," in Optical Fiber Communication Conference/National Fiber Optic Engineers Conference 2013, (2014), Paper Th3A.3.
30. R. Schmogrow, D. Hillerkuss, M. Dreschmann, M. Huebner, M. Winter, J. Meyer, B. Nebendahl, C. Koos, J. Becker, W. Freude, and J. Leuthold, "Real-time software-defined multiformat transmitter generating 64QAM at 28 GBd," IEEE Photon. Technol. Lett. **22**(21), 1601–1603 (2010).

#212650 - $15.00 USD Received 26 May 2014; revised 25 Aug 2014; accepted 23 Dec 2014; published 13 Jan 2015

31. P. Winzer, A. Gnauck, A. Konczykowska, F. Jorge, and J.-Y. Dupuy, "Penalties from in-band crosstalk for advanced optical modulation formats," in 37th European Conference and Exposition on Optical Communications, (Optical Society of America, 2011), Paper Tu.5.B.7.
32. R. Schmogrow, B. Nebendahl, M. Winter, A. Josten, D. Hillerkuss, S. Koenig, J. Meyer, M. Dreschmann, M. Huebner, C. Koos, J. Becker, W. Freude, and J. Leuthold, "Error vector magnitude as a performance measure for advanced modulation formats," IEEE Photon. Technol. Lett. **24**(1), 61–63 (2012).
33. F. Chang, K. Onohara, and T. Mizuochi, "Forward error correction for 100 G transport networks," IEEE Commun. Mag. **48**(3), S48–S55 (2010).
34. B. Li, K. J. Larsen, D. Zibar, and I. Tafur Monroy, "Over 10 dB net coding gain based on 20% overhead hard decision forward error correction in 100G optical communication systems," in 37th European Conference and Exposition on Optical Communications, (Optical Society of America, 2011), Paper Tu.6.A.3.
35. T. Herr, V. Brasch, J. D. Jost, C. Y. Wang, N. M. Kondratiev, M. L. Gorodetsky, and T. J. Kippenberg, "Temporal solitons in optical microresonators," Nat. Photonics **8**(2), 145–152 (2013).
36. V. Brasch, T. Herr, M. Pfeiffer, J. Jost, and T. Kippenberg, "Temporal soliton generation in chip-based silicion nitride microresonators," in Proceedings of CLEO: 2014, (Optical Society of America, 2014), Paper FTh1D.1.

1. Introduction

Interfaces operating at 400 Gbit/s or 1 Tbit/s are foreseen as the next standards after 100 Gbit/s Ethernet [1–3]. In this context, optical super-channels are promising candidates, combining a multitude of sub-channels in a wavelength-division multiplexing (WDM) scheme, while each sub-channel operates at a moderate symbol rate that complies with currently available CMOS driver circuitry. Typically the super-channels use spectrally efficient advanced modulation formats such as quadrature phase shift keying (QPSK) or 16-state quadrature amplitude modulation (QAM) in combination with advanced multiplexing schemes such as orthogonal frequency-division multiplexing (OFDM) [4–6] or Nyquist-WDM [7–10]. The performance of these transmission schemes depends heavily on the properties of the optical source, in particular on the number of lines, the power per line, the optical carrier-to-noise ratio (OCNR), the optical linewidth, and on the relative intensity noise (RIN). In addition, tunability of emission wavelength and line spacing are important features providing flexibility of the transmission scheme. Terabit/s super-channel transmission has been demonstrated before, using different approaches for realizing the optical source. These approaches include ensembles of independent lasers [11,12], single-laser concepts with sidebands generated by external modulation [13,14] or by Kerr comb generation in optically nonlinear high-Q microresonators [15], and fiber-based spectral broadening [5,9,16–18]. Arrays of independent lasers offer flexibility and do not require filters for spectrally separating the comb lines. However, the achievable spectral efficiency (SE) is limited by the drift of the individual emission wavelengths and the associated guard bands. For modulator-based comb sources, the number of comb lines is generally limited by the achievable modulation depth [13] unless complex arrangements of cascaded modulators with synchronized driving signals are used [14,19]. Moreover, if large numbers of lines are to be generated, the power of the comb lines is limited by the power handling capacity and by the insertion loss of the modulator. Kerr comb sources can provide a large numbers of lines, but require sophisticated pumping schemes and the line spacing is inherently tied to the free spectral range of the underlying resonator. Broadband frequency combs for terabit/s super-channels can also be generated by solid-state mode-locked lasers in combination with highly nonlinear fibers [5,9,20], or multi-stage parametric mixers [16–18]. However, both approaches require strong optical pumps and large interaction lengths in delicately arranged sequences of specialized optical fibers. Integration density is hence limited. While this might be acceptable when considering the ultra-high data rates achieved with these sources — several tens of terabit/s — the associated higher power consumption is not very well suited for point-to-point links that require only a limited number of comb lines (order of 10) to form a terabit/s super-channel.

In this work we demonstrate that gain-switched comb sources (GSCS) [21] can be used as an alternative approach to generate terabit/s super-channels. These devices exploit injection locking of a gain-switched laser diode and feature both an electrically tunable free spectral

#212650 - $15.00 USD Received 26 May 2014; revised 25 Aug 2014; accepted 23 Dec 2014; published 13 Jan 2015

range [22] and an electrically tunable center wavelength [23], good spectral flatness, high OCNR, low RIN and low optical linewidth. In Refs [24,25] such a comb source has been used to transmit several channels operating at 10 Gbit/s and 40 Gbit/s, respectively, in a passive optical network (PON) with coherent detection. The spectral efficiency in these experiments amounted to 1 bit/s/Hz and 2 bit/s/Hz, respectively. Here we demonstrate six distinct terabit/s super-channel experiments using polarization division multiplexed (PDM) QPSK and 16QAM in combination with Nyquist pulse shaping for efficient use of the available bandwidth. Transmission over various distances of standard single-mode fiber (SSMF) has been tested. We achieve an aggregate line rate (net data rate) of 1.296 Tbit/s (1.109 Tbit/s) after transmission over 150 km of SSMF in a spectral bandwidth of 166.5 GHz [26]. This corresponds to a (net) spectral efficiency of 7.8 bit/s/Hz (6.7 bit/s/Hz). When combining 16QAM on strong carriers and QPSK modulation on the weaker carriers, the line rate (net data rate) can be boosted to 2.112 Tbit/s (1.867 Tbit/s) and transmitted over 300 km using a bandwidth of 300 GHz.

The paper is structured as follows: In Section 2 we introduce the GSCS concept. The experimental setup for generating and characterizing the terabit/s super-channels is given in Section 3. Section 4 shows the experimental proof of the terabit/s super-channels and discusses the results. In Section 5 we compare the presented results with previous comb-based terabit/s optical data transmission experiments and discuss the potential of the techniques for chip-scale integration. A summary is presented in Section 6.

2. Gain-switched comb source

Figure 1(a) shows the experimental setup of the GSCS. Gain switching is achieved by driving a distributed feedback (DFB) slave laser diode with a large sinusoidal signal (24 dBm) at a frequency that corresponds to the desired line spacing, in combination with a DC bias current of approximately four times the threshold current ($I_{th} \approx 12.5$ mA). Additionally, a master laser

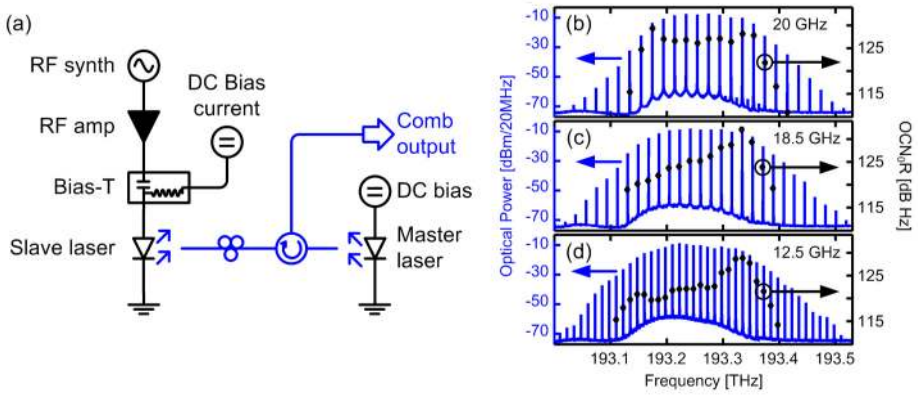

Fig. 1. (a) Setup schematic of the GSCS. A frequency comb is generated by gain switching of the DFB slave laser. The line spacing is determined by the frequency of the RF drive signal. By injecting light from the master laser to the slave laser via a circulator, the low linewidth and RIN of the master laser are transferred to the comb lines. (b-d) Comb spectra (blue, left axis) measured at position "Comb output" with a line spacing of (b) 20 GHz, (c) 18.5 GHz, and (d) 12.5 GHz (RBW 20 MHz) and optical carrier-to-noise density ratio (OCN_0R – black, right axis) for the comb lines used for the data transmission experiments.

(Agilent N7711A) injects continuous-wave light into the slave laser via a polarization controller (PC) and an optical circulator. The master laser establishes coherence between subsequent pulses and transfers its characteristically low optical linewidth (80 kHz) to the individual modes of the comb [21,23], and reduces the RIN of the comb modes [27]. The comb's center wavelength can be tuned by simultaneously adjusting the emission wavelength of the master laser and the temperature of the DFB slave. The polarization controller is used

#212650 - $15.00 USD Received 26 May 2014; revised 25 Aug 2014; accepted 23 Dec 2014; published 13 Jan 2015

to align the polarization state of the injected light with that of the slave laser mode. By carefully selecting the wavelength detuning and the injected power, long-term (during several days) operational stability of the GSCS can be achieved. The GSCS operates without automated feedback control, and without need for manual adjustment of detuning and polarization. In our experiments, the injection power is set to approximately 7 dBm, and the slave laser is temperature-controlled at 25 °C.

We investigate the GSCS with three different line spacings, 20 GHz, 18.5 GHz and 12.5 GHz, by appropriately changing the frequency of the RF synthesizer. The respective GSCS spectra are depicted in Figs. 1(b)–1(d) on the left-hand axis (blue). The power levels correspond to the actual power of the comb measured at position "Comb output" in Fig. 1(a). The total power in all three cases amounts to + 3.5 dBm. On the right-hand axis of Figs. 1(b)–1(d) we depict the optical carrier-to-noise density ratio (OCN_0R) of the comb lines that are used for the data transmission experiments. The OCN_0R is defined by the ratio of the power of the unmodulated carrier to the underlying noise power in a spectral bandwidth of 1 Hz. Note that some authors use a reference bandwidth of 0.1 nm for evaluating the noise power. An OCN_0R value of 125 dB Hz corresponds to an OCNR (by some authors named OSNR) of approximately 24 dB, when measuring the noise in a reference bandwidth of 0.1 nm as done, e. g., in [16,20]. The origin of the noise floor in the GSCS spectra is discussed in [28], where the trade-off between flatness and high-frequency FM noise was elaborated. Here, we concentrate on "flat combs" [28], accepting the noise penalty in favor of a higher number of sub-channels and hence higher aggregate data rates.

Note that the optical bandwidth of all three combs in Figs. 1(b)–1(d) is the same. The bandwidth is dictated by the intrinsic dynamics of photons and electrons within the slave laser. Choosing a smaller line spacing will yield a larger number of lines. With respect to the possible number and the power of lines, the GSCS competes with frequency combs generated with a single electro-optic modulator. The main advantage of the GSCS is its inherent stability without any bias control. Even the polarization of the master laser is uncritical once it is set, because a slight polarization change results in a minor reduction of the locking range only. The temperature control of the master laser would be required anyway for the laser in a modulator-based comb generator. Note that the current setup for comb generation comprises discrete components. Further cost and complexity reduction as well as a stability improvement can be obtained by a monolithic integration of master and slave lasers [29]. For an integrated GSCS, the total power consumption can be estimated to be approximately 10 W, see Table 1. The total optical output power then amounts to typically 3.5 dBm for the entire comb. For some applications, the output power needs to be boosted to values of 10 – 17 dBm per line. This can be achieved by appropriate amplifier stages adding at most 10 W to the total power consumption.

Table 1. Power consumption estimation for a GSCS using integrated components

Component	Estimated power consumption
Two-channel laser driver	0.7 W[a]
Temperature controllers	2 × 1.75 W[b]
RF source	1.3 W[c]
RF amplifier	4.5 W[d]

[a] https://www.hittite.com/products/view.html/view/HMC807LP6CE, assuming both lasers are operated at 80 mA.
[b] http://www.maximintegrated.com/en/products/power/switching-regulators/MAX8520.html
[c] https://www.hittite.com/products/view.html/view/HMC807LP6CE
[d] http://www.shf.de/wp-content/uploads/datasheets/datasheet_shf_100bp.pdf

3. Super-channel generation and characterization

For a given line spacing, super-channel capacity is dictated by two parameters: First, the number of carriers that can be derived from the comb source, which defines the number of

#212650 - $15.00 USD Received 26 May 2014; revised 25 Aug 2014; accepted 23 Dec 2014; published 13 Jan 2015

sub-channels, and second, the power levels and OCNR of the respective carriers that determine the modulation formats to be used on each sub-channel provided that the carrier linewidth is sufficiently low. As a matter of fact, the comb line power is highest in the center of the GSCS spectrum and decreases towards the periphery. In practical transmission systems, however, equal power distribution among all involved sub-channels is desired. This requires attenuation of the center comb lines relative to the power of the outer ones, and subsequent amplification to overcome insertion and modulation losses of the transmitter. The associated amplified spontaneous emission (ASE) noise limits the performance of the entire super-channel and is hence a crucial parameter when designing comb-based transmission systems. In the following experiments, we seek to maximize super-channel performance for a given transmission system, and to investigate the trade-off between spectral efficiency and transmission reach for the case of the GSCS.

The experimental setup to emulate a super-channel transmitter (Tx) and receiver (Rx) is depicted in Fig. 2. We use a programmable filter (Finisar WaveShaper) to equalize the power in the comb lines and to reject outer comb lines that feature too little power for sufficient modulation. The comb lines are then dis-interleaved into two sets of sub-carriers (odd and even). For the 20 GHz and 18.5 GHz line spacing, the dis-interleaving can be directly performed by the programmable filter, while for the 12.5 GHz comb, a commercially available interleaver (Optoplex Corp.) is used. The two sets of sub-carriers are amplified by two nominally identical EDFA operated in constant output power mode set to 16 dBm. Note that the equalization of the comb results in a reduction of the input power to these amplifiers. This limits the flattening of the comb lines as stronger equalization requires higher amplification afterwards, and hence more ASE noise adds to the comb lines. While this has a negative effect on the OCNR of the carriers, it helps to ensure comparable input power levels for the transmission EDFA and at the receiver input, so that the various transmission experiments can be compared.

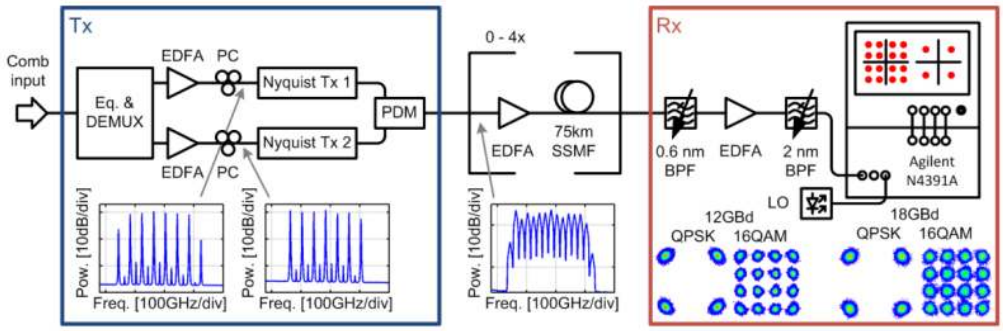

Fig. 2. Schematic of the GSCS terabit/s super-channel transmitter and coherent receiver. The frequency comb is equalized and de-multiplexed into odd and even comb lines. The two sets of carriers are amplified, modulated with independent, sinc-shaped Nyquist signals and then combined in a polarization division multiplexing (PDM) scheme. Insets show the optical spectra measured using a 0.01 nm resolution bandwidth. The super-channel is either sent directly to the receiver or transmitted through up to four spans of 75 km standard single mode fiber (SSMF) with an EDFA before each span. At the receiver, the desired sub-channel is selected by a band-pass filter (BPF), amplified and coherently detected using a narrow-linewidth laser as a local oscillator (LO). The signal is recorded and analyzed using an optical modulation analyzer (Agilent N4391A). The presented constellation diagrams are obtained using an ECL as a carrier, and serve as reference measurements. The phase error that can be particularly seen in the 12 GBd constellation diagrams as well as the stronger noise cloud for the 18 GBd measurements is attributed to our transmitter hardware.

The two sub-carrier sets are then independently modulated using an IQ modulator driven by band-limited Nyquist pulses that are generated by a proprietary multi-format transmitter (Nyquist-Tx) [8,30]. Polarization division multiplexing (PDM) is emulated by splitting the

#212650 - $15.00 USD Received 26 May 2014; revised 25 Aug 2014; accepted 23 Dec 2014; published 13 Jan 2015

combined outputs of the two Nyquist-Tx into two paths, which are recombined after different delays to form two orthogonal polarization states in a SSMF. The insets show exemplary optical spectra, RBW 0.01 nm, of the separate sub-carrier sets and the combined terabit/s data stream for the case of the 20 GHz comb and 18 GBd QPSK modulation. When using the waveshaper for dis-interleaving and flattening, we find that the crosstalk, i. e., the ratio of the power of a comb line at its allocated waveshaper output port and the residual power of the same comb line at the other output port is actually a function of the attenuation supplied to this particular comb line. We find crosstalk attenuation levels of (19.9 ± 4.4) dB for the QPSK and (29.1 ± 6.4) dB for the 16QAM experiments. We do not observe a correlation between crosstalk attenuation and the performance of the sub-channels, and hence conclude that our results are not limited by crosstalk effects, This finding is in accordance to the one reported in [31], where a SNR penalty of less than 1 dB is predicted for these levels of crosstalk.

The super-channels were either sent directly to the Rx for back-to-back (B2B) characterization, or transmitted over up to four spans of 75 km SSMF with an erbium-doped fiber amplifier (EDFA) before each span. The launch power into the transmission fibers has been set to approximately –3dBm per sub-channel, providing a good compromise between nonlinear signal impairments and noise. As a local oscillator (LO) we use an external cavity laser (ECL) specified with a linewidth less than 100 kHz. The signals were analyzed using an optical modulation analyzer (Agilent N4391A) and with offline processing. We perform digital brick-wall filtering, polarization demultiplexing, dispersion compensation, and adaptive equalization before evaluating the bit-error-ratio (BER) and the error vector magnitude (EVM_m) of each sub-channel individually. The EVM subscript "m" indicates the normalization of the EVM to the maximum power of the longest ideal constellation vector.

As a performance measure of the system we test both modulation paths individually with a narrow-linewidth ECL that is comparable to the ECL used as local oscillator. With 18 GBd modulation we achieve an average EVM_m of 10.5% and 9.8% for QPSK and 16QAM, respectively, while an average EVM_m of 8.5% and 7.5% is obtained for 12 GBd modulation, respectively. The dependence of the performance on symbol rate is attributed to the limited bandwidth of our anti-aliasing filters after digital-to-analog conversion.

Assuming that the signal is impaired by additive white Gaussian noise only, a direct relation from the EVM_m to the BER can be established [32]. In our experiments this assumption is not perfectly fulfilled as the constellations show a small signature of phase noise. As we see this behavior also for the reference measurements with an ECL, see insets in Fig. 2, we attribute this to our transmitter hardware rather than to the linewidth of the optical source. Nevertheless we present our results using the EVM_m metric, since for the QPSK experiments we generally did not measure a high-enough number of errors within the length of one recording. For the 16QAM experiments we give both the EVM_m and the BER. One can see that the EVM_m slightly overestimates the signal quality, which we attribute to the small phase error introduced by our transmitter hardware as well as the fact that our EVM_m measurement is non-data-aided while the relation in [32] assumes a data-aided measurement of the EVM_m.

Another interesting metric would be the sub-channel OSNR. However, such an evaluation is not easily possible in our de-multiplexer setup: Due to narrowband filtering of the individual comb lines using a passband width of the order of 10 GHz, the filtered ASE background is strongly non-uniform, and we can hence not any more estimate the noise power density at the carrier wavelength from a measurement taken in the center between two carriers. We may, however, estimate the sub-channel OSNR from the OCN_0R measured at the output of the GSCS. For the 20 GHz comb, the OCN_0R is relatively uniform and amounts to approximately 127 dB Hz, which would translate into an OSNR of roughly 26 dB in a reference bandwidth of 0.1 nm after modulation and back-to-back reception.

#212650 - $15.00 USD Received 26 May 2014; revised 25 Aug 2014; accepted 23 Dec 2014; published 13 Jan 2015

4. Experimental results

4.1 Experimental parameters and comparison of super-channels

We investigate six different super-channel architectures that are based on three different line spacings, 20 GHz, 18.5 GHz and 12.5 GHz, and two different modulation formats, QPSK and 16QAM. The results of all six experiments are summarized in Table 2. For each super-channel we take as many comb lines as possible, each carrying a Nyquist-WDM sub-channel. Comb lines that were too weak for the respective modulation format were suppressed by the equalization filter (equalizer "Eq." in Fig. 2) prior to recording the data presented here. For the super-channels that were derived from the 20 GHz and the 18.5 GHz comb we use a symbol rate of 18 GBd and hence obtain a sub-channel line rate of 72 Gbit/s for PDM-QPSK modulation and 144 Gbit/s for PDM-16QAM. A symbol rate of 12 GBd was used for the super-channels based on the 12.5 GHz comb leading to a sub-channel line rate of 48 Gbit/s and 96 Gbit/s for the two modulation formats employed. For all symbol rates, the clock rate of the digital-to-analog converters (DAC) of the Nyquist-Tx was kept constant at 24 GHz, while the oversampling factor q for generating the sinc-shaped output pulses was adapted to $q = 4/3$ for 18 GBd and $q = 2$ for 12 GBd.

Table 2. Summary of all super-channels

Line spacing [GHz]	Modulation format	No. of sub-ch.	Sub-ch. line rate [Gbit/s]	Aggr. line rate [Tbit/s]	Occupied bandwidth [GHz]	Net aggr. data rate [Tbit/s]	Net SE [bit/s/Hz] (transm. dist.)
20	PDM-QPSK	13	72	0.936	260	0.875	3.4 (300 km)
	PDM-16QAM	8	144	1.152	160	1.047	6.5 (150 km)
18.5	PDM-QPSK	15	72	1.080	277.5	1.009	3.6 (300 km)
	PDM-16QAM	9	144	1.296	166.5	1.109	6.7 (150 km)
12.5	PDM-QPSK	24	48	1.152	300	1.077	3.6 (300 km)
	PDM-QPSK/ PDM-16QAM	4 / 20	48 / 96	2.112	300	1.867	6.2 (300 km)

In Table 2, the aggregate line rate is obtained by multiplication of the number of sub-channels with the sub-channel line rate, and the bandwidth of the super-channel is given by the product of sub-channel number with the comb line spacing. For calculating the net aggregate data rate one needs to take into account the overhead for forward error correction (FEC). FEC schemes with 7% overhead can cope with BER of up to 4.5×10^{-3} [33], a requirement which was fulfilled for all B2B experiments. For some transmission experiments, this BER threshold is exceeded as discussed in the subsequent sections. In these cases, some of the sub-channels require more advanced FEC codes with a larger overhead of, e.g. 20%, having a higher BER limit of, e.g., 1.5×10^{-2} [34]. We calculate the net aggregate data rate for each super-channel after the longest tested transmission distance by taking into account the respective overhead for each sub-channel individually. The net SE is then calculated from the ratio of the net aggregate data rate and the occupied bandwidth. In the parenthesis we indicate the actual fiber transmission distance over which this spectral efficiency has been achieved.

4.2 Terabit/s super-channels with an 18.5 GHz comb

For the highest spectral efficiency we operate the Nyquist-Tx at a symbol rate of 18 GBd and choose a comb line spacing of 18.5 GHz, see spectrum of Fig. 1(c). We select a total of 15 lines using the equalization filter and flatten the spectrum to the level of the weakest carrier. Figure 3(a) shows the spectrum of the super-channel using PDM-QPSK modulation with a total aggregate line rate of 1.08 Tbit/s, measured in a resolution bandwidth of 0.01 nm. For each sub-channel the measured EVM_m, averaged over both polarizations, is presented in Fig. 3(b) for the B2B case and for transmission distances of 75 km, 150 km, 225 km, and 300 km.

#212650 - $15.00 USD Received 26 May 2014; revised 25 Aug 2014; accepted 23 Dec 2014; published 13 Jan 2015

The transmission lengths are distinguished by different symbols, colors, and by an offset in the horizontal direction. Note that we could not find enough errors in the recorded number of 4,500,000 bits for evaluating the BER reliably. Therefore we conclude that the BER of all sub-channels are clearly below the threshold for second-generation forward-error correction

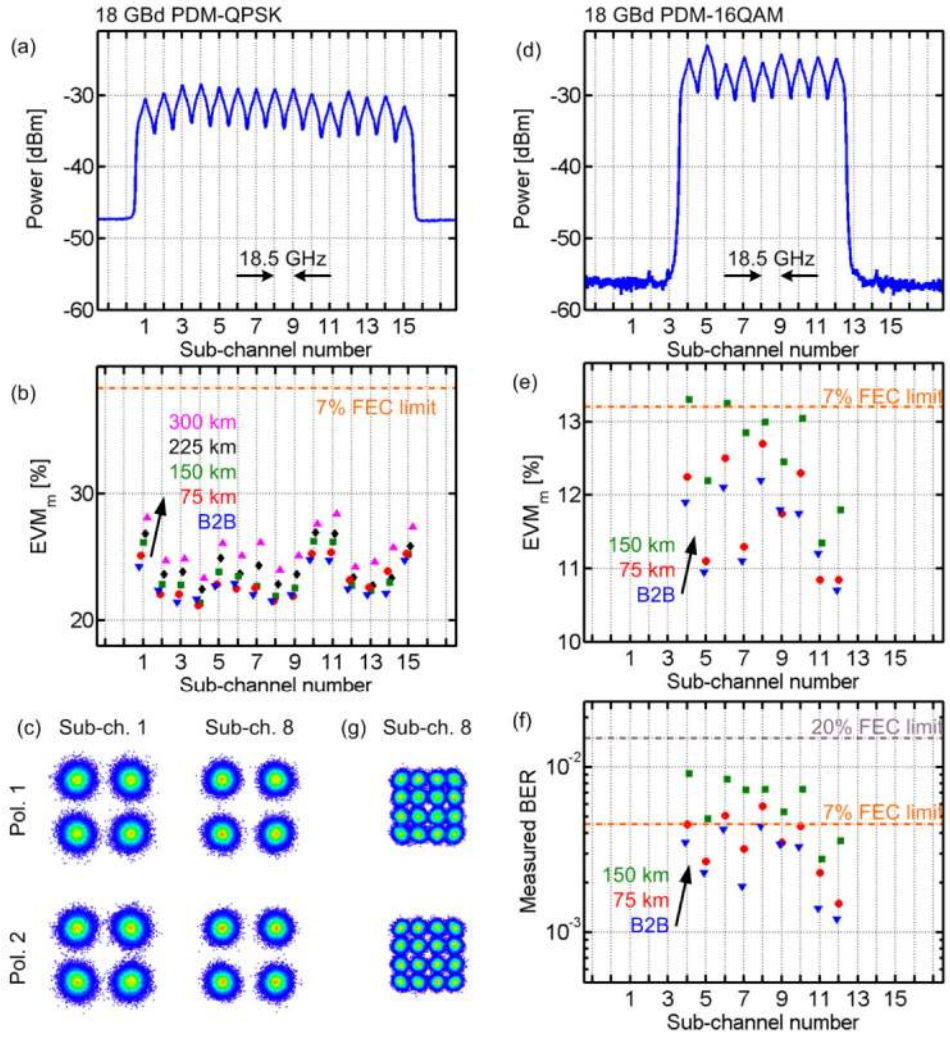

Fig. 3. Spectra, signal quality and constellations for super-channel transmission with an 18.5 GHz comb. Left column for QPSK, right column for 16QAM. (a) Spectrum of the super-channel derived from a 18.5 GHz comb with 18 GBd PDM-QPSK modulation (RBW 0.01 nm). The sub-channel number increases with carrier frequency. (b) Measured EVM_m for each sub-channel and transmission over different distances. We find that all 15 sub-channels perform better than the threshold for second-generation FEC with 7% overhead, yielding a total data rate of 1.009 Tbit/s transmitted over 300 km. (c) Measured constellation diagrams for sub-channels 1 and 8 of the PDM-QPSK experiment. (d) Spectrum of the super-channel derived from a 18.5 GHz comb with 18 GBd PDM-16QAM (RBW 0.01 nm). (e-f) Measured EVM_m and BER for each sub-channel and transmission over different distances. We find that 2 (7) sub-channels perform better than the FEC threshold with 7% (20%) overhead, yielding a aggregate net data rate of 1.009 Tbit/s transmitted over 150 km. (g) Measured constellation diagrams for sub-channel 8 of the PDM-16QAM experiment.

(FEC) with 7% overhead, given by a BER of 4.5×10^{-3}, which corresponds to an EVM_m of 38.3% [32]. We hence obtain a net super-channel capacity of 1.009 Tbit/s in a bandwidth of

#212650 - $15.00 USD Received 26 May 2014; revised 25 Aug 2014; accepted 23 Dec 2014; published 13 Jan 2015

278 GHz, corresponding to a net spectral efficiency of 3.6 bit/s/Hz. Selected constellations diagrams of the B2B-experiments are displayed in Fig. 3(c). We compare two sub-channels, one at the border and one at the center of the super-channel spectrum. They perform similar for both polarizations.

The bandwidth requirement can be reduced by a factor of two when upgrading the system from QPSK to 16QAM signaling. This doubles the line rate per channel but requires a higher optical signal-to-noise-ratio (OSNR). To this end we increase the equalization power level for flattening the comb, i. e., the average attenuation is decreased, which leads to carriers with a higher power. However, only fewer comb lines contribute the required power, hence the number of sub-channels is reduced from 15 to 9. Because a higher power level is input to the EDFA, the amplification and the ASE contribution is lower, leading to a larger OCNR. Additionally, the smaller attenuation results in a reduced crosstalk of the waveshaper, see Section 3, third paragraph. Spectrum, EVM_m and measured BER are presented in Figs. 3(d)–3(f). For short transmission distances (B2B), the BER stays below the standard FEC limit for 7% overhead. For a transmission distance of 150 km, seven of the nine sub-channels exceed the BER mark for standard FEC, and implementations with larger overhead, i. e., 20% overhead, become necessary. The remaining two sub-channels fall below the FEC threshold with 7% overhead even after transmission over 150 km. The aggregate line rate (net data rate) of this super-channel amounts to 1.296 Tbit/s (1.109 Tbit/s), corresponding to a (net) spectral efficiency of 7.8 bit/s/Hz (6.7 bit/s/Hz). This is among the highest values achieved for 16QAM in terabit/s super-channels.

In Fig. 3(g) we show the constellation diagram of the central sub-channel 8 in two polarizations. Note that the smaller noise clouds as compared to Fig. 3(c) (QPSK) for the same sub-channel is a direct consequence of the higher power level of the flattened comb lines in the 16QAM case, which yields a higher OSNR of all sub-channels.

4.3 Terabit/s super-channels with a 20 GHz comb

A more robust super-channel can be generated by increasing the guard band. To this end, we increase the line spacing of the comb to 20 GHz, see spectrum in Fig. 1(b), while keeping the same symbol rate at the Nyquist-Tx. We select again 15 comb lines, 13 of which we flatten to the same power level as in the 18.5 GHz experiment for better comparison. The outermost carriers do not reach this power level and hence their performance drops below that of the inner 13 carriers. This can be seen in the spectrum as well as in the EVM_m results for QPSK modulation, Figs. 4(a) and 4(b). Taking into account the inner 13 sub-channels, the super-channel aggregate line rate (net data rate) amounts to 0.936 Tbit/s (0.875 Tbit/s), with a (net) spectral efficiency of 3.6 bit/s/Hz (3.4 bit/s/Hz).

Selected constellations diagrams of the B2B-experiments are displayed in Fig. 4(c). We compare two sub-channels, one at the border of the comb (sub-channel 1, also representative for sub-channel 15), and the central sub-channel 8 (representative for sub-channels 2 to 14). Sub-channels 1 and 15 suffer from low carrier power and therefore from a small OSNR. However, the central sub-channels 2 to 14 have an EVM_m which is slightly better than that of the corresponding sub-channels of the 18.5 GHz experiment. We attribute this to the larger guard band that reduces inter-channel interference originating from imperfect Nyquist pulse shaping.

This fact becomes even more evident when comparing the 16QAM 20 GHz comb experiment Figs. 4(d)–4(f) with the 18.5 GHz comb experiment in Figs. 3(d)–3(f). We achieve 6 (2) sub-channels that are better than the 7% (20%) FEC limit after 150 km of fiber transmission. The aggregate line rate (net data rate) amounts to 1.152 Tbit/s (1.047 Tbit/s). The (net) spectral efficiency amounts to 7.2 bit/s/Hz (6.5 bit/s/Hz). These results must be compared to the case of the 18.5 GHz comb and illustrate the trade-off between super-channel capacity and reach: For a comparable capacity, we used 9 sub-channels, but only 2 (7) were better than the 7% (20%) FEC limit after transmission over 150 km. We conclude that

#212650 - $15.00 USD Received 26 May 2014; revised 25 Aug 2014; accepted 23 Dec 2014; published 13 Jan 2015

transmission with the 20 GHz comb has the larger capacity for a reach, where the channels with a FEC overhead of 20% would drop out.

In Fig. 4(g) we show the constellation diagram of the central sub-channel 8 in two polarizations. The smaller noise clouds as compared to Fig. 4(c) (QPSK) for the same sub-channel follow from the higher power level of the flattened comb, see Figs. 3(c) and 3(g).

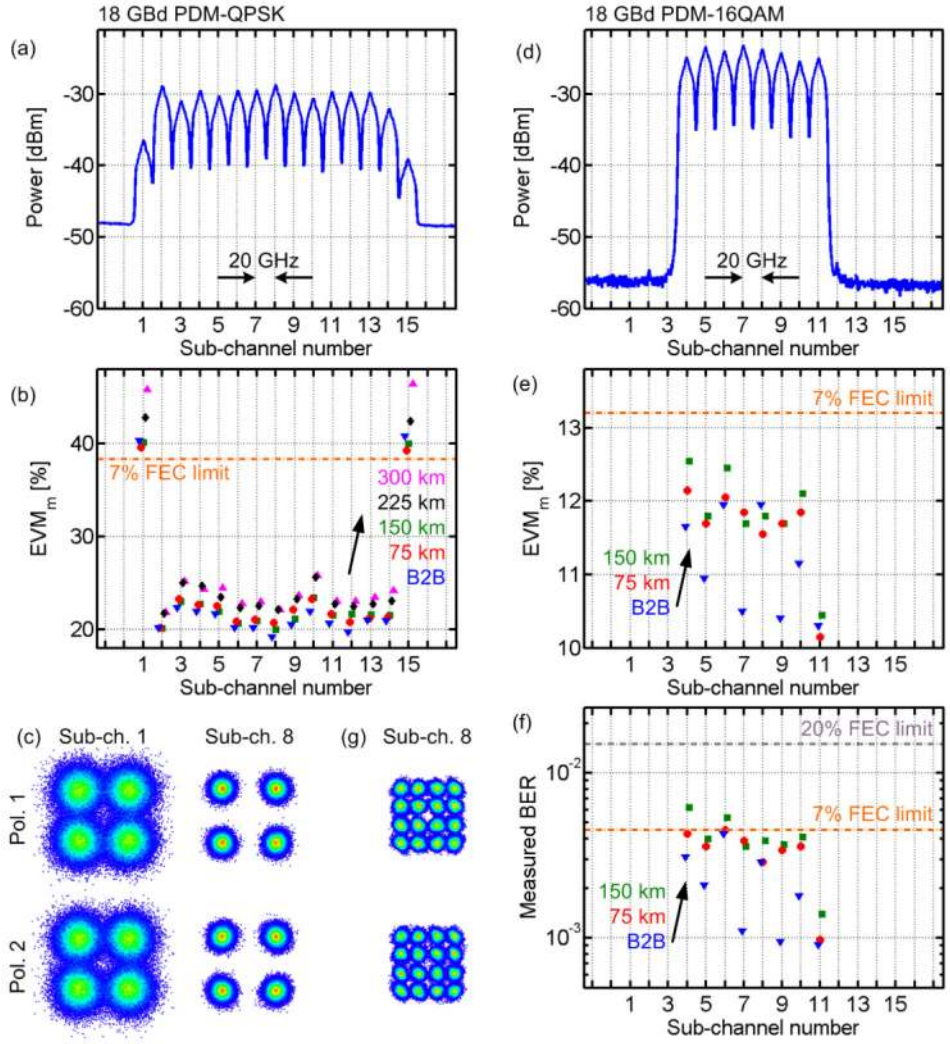

Fig. 4. Spectra, signal quality and constellations for super-channel transmission with a 20 GHz comb. Left column for QPSK, right column for 16QAM. (a) Spectrum of the super-channel derived from a 20 GHz comb with 18 GBd PDM-QPSK modulation (RBW 0.01 nm). The sub-channel number increases with carrier frequency. (b) Measured EVM_m for each sub-channel and transmission over different distances. We find that 13 sub-channels perform better than the threshold for second-generation FEC with 7% overhead, yielding a total data rate of 0.875 Tbit/s transmitted over 300 km. (c) Measured constellation diagrams for sub-channels 1 and 8 of the PDM-QPSK experiment. (d) Spectrum of the super-channel derived from a 18.5 GHz comb with 18 GBd PDM-16QAM (RBW 0.01 nm). (e-f) Measured EVM_m and BER for each sub-channel and transmission over different distances. We find that 6 (2) sub-channels perform better than the FEC threshold with 7% (20%) overhead, yielding a total data rate of 1.047 Tbit/s transmitted over 150 km. (g) Measured constellation diagrams for sub-channel 8 of the PDM-16QAM experiment.

#212650 - $15.00 USD Received 26 May 2014; revised 25 Aug 2014; accepted 23 Dec 2014; published 13 Jan 2015

4.4 Terabit/s super-channels with a 12.5 GHz comb

In a last set of experiments, we take advantage of the tunability of the GSCS by adapting the line spacing and center frequency to the 12.5 GHz ITU-grid, see spectrum in Fig. 1(d). This enables the use of a commercial fixed interleaver to separate odd and even sub-carriers. The interleaver exhibits an excellent extinction of the odd carriers in the path of the even carriers, and vice versa. The programmable filter is then used for equalization only.

For the QPSK experiments, we use again the same equalization level as for the 18.5 GHz and the 20 GHz comb while reducing the symbol rate to 12 GBd. This leads to 24 sub-channels with EVM_m values well below the 7% FEC limit, see Fig. 5(a) for the super-channel spectrum and Fig. 5(b) for the EVM_m results. The four outermost channels do not reach the power level which was used for flattening, and hence drop in performance. The (net) capacity of this super-channel is 1.152 Tbit/s (1.077 Tbit/s), and the (net) spectral efficiency amounts to 3.8 bit/s/Hz (3.6 bit/s/Hz). Figure 5(c) shows selected constellation diagrams for the QPSK experiment in the B2B case. The constellation diagrams represent peripheral (example: sub-channel 1) and central sub-channels (example: sub-channel 12), respectively.

We finally boost the super-channel aggregate line rate to 2.112 Tbit/s by increasing the equalization level and by admitting the weak outer comb lines, too. This enables 16QAM modulation on 20 sub-channels in the center, while 4 of the outer sub-channels still enable QPSK operation below the 7% FEC threshold, see Figs. 5(d)–5(f). The aggregate net data rate amounts to 1.867 Tbit/s with a net spectral efficiency of 6.2 bit/s/Hz for transmission over 300 km. Figure 5(g) shows the PDM-16QAM constellation diagram of a central 16QAM sub-channel.

Comparing the performance of the individual sub-channels for both super-channels with the 12.5 GHz GSCS it is possible to observe a slight reduction of the EVM_m and the BER with increasing sub-channel number. This performance dependence on the sub-channel number seems to be correlated with the variations of the OCN_0R of the comb lines as shown in Fig. 1(d). Note that, also the 18.5 GHz GSCS exhibits strong variations of the OCN_0R, but they do not seem to be correlated with the respective EVM_m. We believe that in contrast to operation at a symbol rate of 12 GBd, the cut-off frequency of the anti-aliasing filters becomes effective at the present symbol rate of 18 GBd (as explained in Section 3 Paragraph 5), and this dominates the OCN_0R-related performance degradation.

#212650 - $15.00 USD Received 26 May 2014; revised 25 Aug 2014; accepted 23 Dec 2014; published 13 Jan 2015

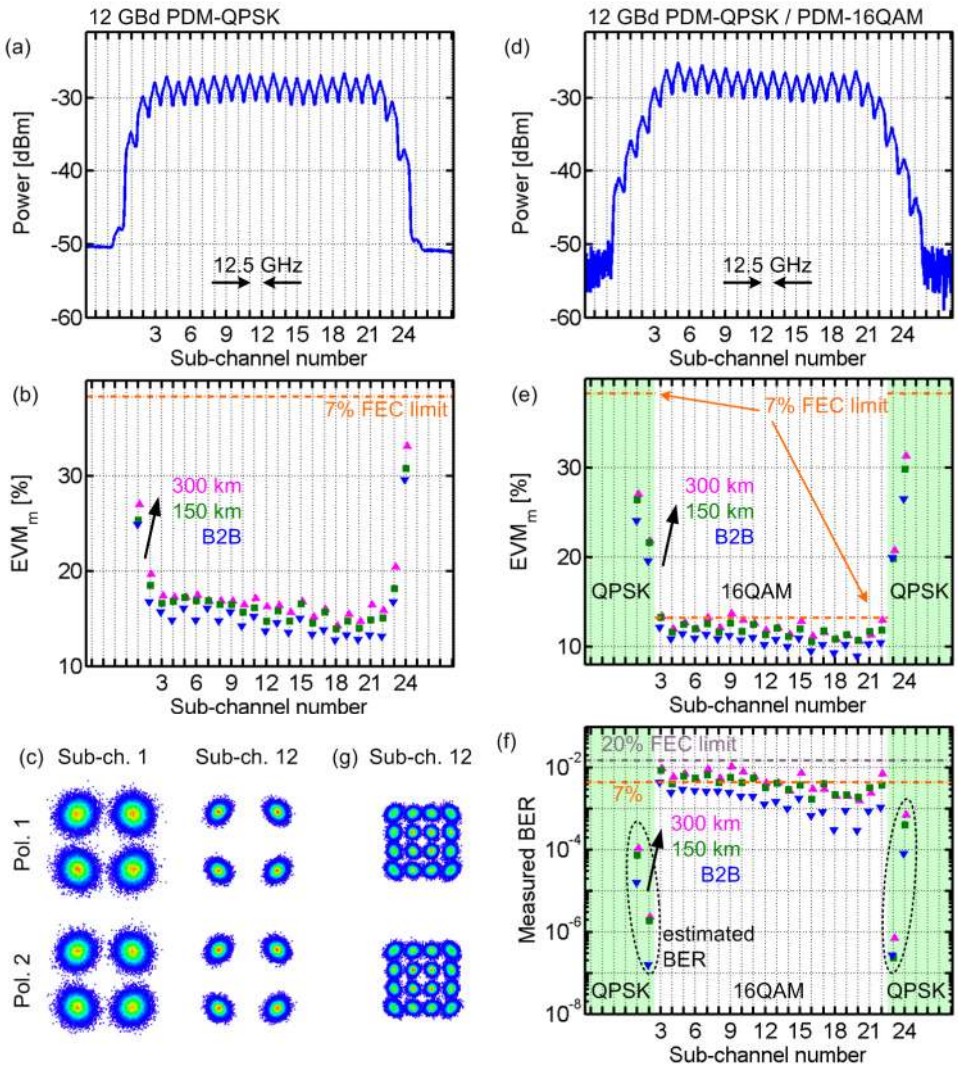

Fig. 5. Spectra, signal quality and constellations for super-channel transmission with a 12.5 GHz comb. Left column for QPSK, right column for mixed QPSK / 16QAM. (a) Spectrum of the super-channel derived from a 12.5 GHz comb with 12 GBd PDM-QPSK modulation (RBW 0.01 nm). The sub-channel number increases with carrier frequency. (b) Measured EVM_m for each sub-channel and transmission over different distances. We find that all 24 sub-channels perform better than the threshold for second-generation FEC, yielding a total data rate of 1.077 Tbit/s transmitted over 300 km. (c) Constellation diagrams for the sub-channels 1 and 12. (d) Spectrum of the super-channel derived from a 12.5 GHz comb with 12 GBd PDM-16QAM (RBW 0.01 nm). (e-f) Measured EVM_m and BER for 12 GBd PDM-16QAM on the inner comb lines (white background) and PDM-QPSK on the outer lines (green background), again for different propagation distances. We find that 13 (11) sub-channels (9 (11) channels using PDM-16QAM and 4 channels using PDM-QPSK) perform better than the threshold for FEC with 7% (20%) overhead, yielding a total data rate of 1.867 Tbit/s, transmitted over 300 km. (g) Measured constellation diagrams for sub-channel 12 of the PDM-QPSK / PDM-16QAM experiment.

5. Comparison with previous Tbit/s experiments using chip-scale comb sources

For chip-scale integration of a Tbit/s transmitter module using an optical frequency comb source it is desirable to co-integrate the comb source together with filters and modulators. In

#212650 - $15.00 USD Received 26 May 2014; revised 25 Aug 2014; accepted 23 Dec 2014; published 13 Jan 2015

this section we provide a comparison of comb generation concepts that have the potential for chip-scale integration, and were already used for Tbit/s super-channel transmission.

Besides the GSCS, several coherent terabit/s data transmission employing other frequency comb generator schemes were previously demonstrated. Some demonstrations use electro-optic modulators that can, for example, be integrated on a silicon-on-insulator chip [13]. Other techniques employ Kerr frequency comb generation in a nonlinear high-Q silicon nitride microresonator [15]. Table 3 summarizes key parameters of these experiments, and compares them with the GSCS data. In lines 1 – 6 of the table, we summarize the results obtained from the same setup as shown in Fig. 2, using the same pulse shape and an identical symbol rate, namely Nyquist-WDM with a symbol rate of 18 GBd. In all these experiments, aggregate line rates of 1 Tbit/s or more were achieved, using up to 20 spectral lines. The specified data relate only to those comb lines that were actually used for Tbit/s transmission. The ranges refer to the minimum and maximum quantities, respectively.

Table 3. Comparison of frequency comb generators for Tbit/s data transmission

	Comb generator type	Line spacing [GHz]	number of lines	Power per line [dBm]	OCN_0R [dB Hz]	Aggregate line rate [Tbit/s]	Ref.
1	GSCS	20	13	–28.2 …–7.1	117 … 129	0.936	
2	GSCS	20	8	–10.7 …–7.1	126 … 128	1.152	This
3	GSCS	18.5	15	–25.7 …–8.0	119 … 132	1.080	work
4	GSCS	18.5	9	–11.4 …–8.0	122 … 132	1.296	
5	Kerr comb	25	20	–32.3 …–5.2	112 … 139	1.440	[15]
6	SOH modulator	25	9	–34.7 …–17.1	117 … 135	1.152	[13]
7	Casc. $LiNbO_3$ Mod	6.48	20	N.A.	N.A.	1.2	[14]
8	2 PM in RFS	25	112	~–15 … 0	>120	11.2	[6]
9	Parametric comb	6.25	1520	N.A.	~120	31.8	[18]
10	MLL + HNLF	12.5	325	N.A.	119 … 141	32.5	[9]

For all these comb sources, a line spacing of the order of 20 GHz was used, which allows both an easy dis-interleaving and a high spectral efficiency. For a data rate in the terabit range, either a PDM-QPSK format was used with 13 to 20 comb lines, or a PDM-16QAM format with 8 or 9 lines. The GSCS shows the best comb uniformity at an acceptable average power level, which is only surpassed by a few lines of the Kerr comb. With respect to the OCN_0R, the GSCS shows the best uniformity, but its average value is smaller than for the other two approaches.

It has to be noted that all three comb sources listed in Table 3, lines 1 to 6, are not yet fully optimized. Further steps towards a hybrid or even a monolithic integration are currently being investigated, and performance improvements are to be expected for all comb generation concepts. For the case of the GSCS it is possible to monolithically integrate two lasers, where the master laser synchronizes the slave laser by injecting light at the back facet of the slave, while the comb is collected from its front facet. This removes the need for a circulator and a polarization controller as in Fig. 1.

The SOH comb generator is a promising approach, since it also allows for easy adjustment of center frequency and line spacing of the comb. Moreover, the underlying modulators feature very low V_π and can thus generate a reasonably large number of comb lines with moderate RF driving powers. It has been shown in [13] that a dual-drive SOH modulator can be used to generate a flat comb with seven lines within 2 dB, whereas the data transmission results listed here still stem from a single-drive modulator. As with any modulator-based approach it is possible to achieve a higher number of lines either by cascading multiple modulators [14] or by placing the modulator(s) into a loop [6]. Lines 7 and 8 of Table 3 show the results obtained for frequency comb generation based on cascaded modulators. The former experiment relies on a multi-core transmission fiber and demonstrates net data rates of 1.12 Tbit/s per core by using orthogonal frequency division multiplexing. The latter experiment used two cascaded phase modulators (PM) in a recirculating frequency shifter (RFS) and

#212650 - $15.00 USD Received 26 May 2014; revised 25 Aug 2014; accepted 23 Dec 2014; published 13 Jan 2015

shows transmission of an OFDM data stream over 640 km SSMF with a net capacity of 10 Tbit/s.

The Kerr frequency comb listed in Table 3 suffers from large line-to-line power variations, which limit the number of available channels and hence the achievable data rate. In the future, this limitation can be overcome by generating so-called soliton combs. Soliton combs have recently been demonstrated with crystalline resonators [35], and evidence of soliton combs has been also found in silicon-nitride resonators [36]. Further advances in fabrication processes will also help reducing the pump power.

The GSCS as well as the silicon-organic hybrid (SOH) modulator-based comb generators excel by a tunable line spacing, which is fixed for Kerr frequency combs by design. On the other hand, Kerr frequency combs can be very broad, and spectral line spacings can be in the order of hundreds of GHz, a range that is not easily accessible with other approaches.

For comparison, lines 8 to 10 of Table 3 give reference data on experiments that achieved multi-Tbit/s data transmission. For the cases of lines 9 and 10, the experiments were conducted using parametric comb generators that exploit Kerr nonlinearities in optical fibers, cf [18]. and [9], respectively. Using two interleaved 12.5 GHz combs generated by multi-stage parametric mixing, data transmission on 77 carriers was demonstrated. Extrapolating the performance of these carriers to the ensemble of 1520 carriers, a total data rate of 31.8 Tbit/s was estimated. Previously, transmission of 32.5 Tbit/s was demonstrated using 325 carriers generated by a solid state mode-locked laser along with spectral broadening in a highly nonlinear fiber. These experiments demonstrate the immense potential of parametric frequency comb generation in conventional systems consisting of discrete elements. Transferring this performance to chip-scale systems could, e.g., be achieved by using soliton Kerr frequency combs [35] and is the goal of ongoing research activities.

6. Summary

In summary, we show that GSCS are well suited for terabit/s super-channel generation. We investigate six different super-channel architectures with different carrier spacings and modulation formats, and evaluate their performance for transmission over different distances. The highest (net) spectral efficiency, 7.8 bit/s/Hz (6.7 bit/s/Hz), is obtained for a GSCS with a carrier spacing of 18.5 GHz and 18 GBd PDM-16QAM, transmitted over 150 km. The data capacity transmitted over 300 km of SSMF can be increased to 1.867 Tbit/s by reducing the line spacing along with the symbol rate and by adapting the modulation format to the OSNR performance of the respective sub-channel. Finally, we presented a comparison between optical frequency comb sources that are suitable for terabit/s super-channel systems, and could be hybridly or monolithically integrated into a chip-scale transmitter module.

Acknowledgments

This work was supported by the EU project “Big Pipes”, by the Center for Functional Nanostructures (CFN) of the Deutsche Forschungsgemeinschaft (DFG) (project A 4.8), by the ERC Starting Grant “EnTeraPIC”, number 280145, by the Karlsruhe School of Optics & Photonics (KSOP), by the Helmholtz International Research School for Teratronics (HIRST), by the Alfried Krupp von Bohlen und Halbach Foundation, by the Initiative and Networking Fund of the Helmholtz Association, by the Higher Education Authority (HEA) PRTLI 4 and 5 INSPIRE Programs, Science Foundation Ireland (SFI CTVR) (10/CE/I1853) and Irish Photonic Integration Centre (IPIC) (12/RC/2276) projects, by the China Scholarship Council, and by Pilot Photonics. We further acknowledge support by the Open Access Publishing Fund of Karlsruhe Institute of Technology (KIT).

#212650 - $15.00 USD Received 26 May 2014; revised 25 Aug 2014; accepted 23 Dec 2014; published 13 Jan 2015